JOC The Journal of Organic Chemistry

Article

pubs.acs.org/joc

Unravelling the Reaction Mechanism of the Reductive Ring Contraction of 1,2-Pyridazines

Pedro J. Silva*

REQUIMTE/Fac. de Ciências da Saúde, Universidade Fernando Pessoa, Rua Carlos da Maia, 296, 4200-150 Porto, Portugal

Supporting Information

ABSTRACT: Substituted pyrroles may be synthesized from selected 1,2-pyridazines through a reductive ring contraction involving the addition of four electrons and four protons. Our density functional theory computations of this reaction mechanism show that the first reduction event must be preceded by the uptake of one proton by 1,2-pyridazine and that the reaction proceeds through a $2e^-/3H^+$-bearing intermediate. In the absence of electron-withdrawing groups able to resonate charge away from the ring, this intermediate lies too high in energy, making the reaction sequence thermodynamically inaccessible. After another two-electron reduction and the addition of two more protons, the original 1,2-pyridazine ring opens. Ring contraction and ammonia elimination then proceed with very small barriers, irrespective of the substituents present in the original 1,2-pyridazine. By establishing the need for electron-withdrawing resonant groups in the 3- and 6-positions to stabilize the critical intermediate in the initial stages of the reaction, this work suggests that the scope of the reductive ring contraction of 1,2-pyridazines may be expanded to pyridazines bearing $COCH_3$ groups, amides or aryls in these positions. We also explain the lack of reactivity of unsubstituted 1,2-pyridazine and analyze the feasibility of bypassing the high energy $2e^-/3H^+$-intermediate through disproportionation of earlier $2e^-/2H^+$-bearing intermediates.

INTRODUCTION

Many different strategies for the synthesis of substituted pyrroles are currently available, ranging from the classical Knorr,[1] Hantszch,[2] and Paal–Knorr[3,4] syntheses to multiple-component palladium-catalyzed reactions[5] and several different methodologies involving the contraction of larger heterocyclic rings.[6] The most widely used of these ring contraction strategies is the reductive contraction of substituted 1,2-pyridazines (**I**) to yield 3,4-substituted pyrroles (**III**) first used by Kornfeld et al.[7] and widely studied[8] and popularized by Boger (Scheme 1). This zinc/acetic acid-catalyzed reaction is

Scheme 1

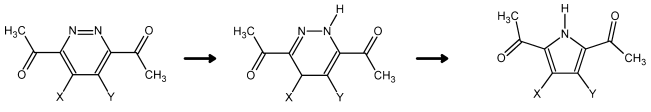

very tolerant of additional functionality around the ring (such as aryl methyl ethers, aryl benzyl ethers, ketones, esters, and carbamates) and has been used in a large number of total syntheses of biologically active natural compounds such as roseophilin,[9] ningalin D,[10] and lycogarubin C.[11,12] Electrochemical investigation[13,14] of this four-electron reaction has shown that the mechanism may involve the formation of a 1,4-dihydropyridazine intermediate (**II**), which is sometimes stable enough to be isolated.[9] The reaction has been reported to proceed more smoothly when using trifluoroacetic acid instead of acetic acid,[9] but neither the precise order of reduction/protonation steps nor the characteristics of the rate-determining steps or the influence of ring substituents have been elucidated. In this work, we have studied the reaction mechanism using computational methods and analyzed the influence of substituents on the 3- and 6-position of the pyridazine ring on the reaction profile. The results allow us to explain the reaction mechanism and understand the influence of pyridazine substituents on reaction rates and the lack of reactivity of unsubstituted 1,2-pyridazine.

COMPUTATIONAL METHODS

The geometries of every organic molecule described were optimized at the B3LYP[15−17] level with the 6-31+G(d) basis set, using autogenerated delocalized coordinates.[18] Accurate DFT energies of the optimized geometries were then calculated using the 6-311+G-(3d,2p) basis set. Zero-point and thermal effects on the energies at 298 K were computed at the optimized geometries using a scaling factor of 0.9804. For the zinc clusters, the Stevens–Basch–Krauss–Jasien pseudopotential[19] (and associated basis set) was used. All computations were performed with the Firefly[20] quantum chemistry package, which is partially based on the GAMESS (US)[21] source code. Deprotonation energies in this work are $G_{base} - G_{acid}$ and therefore do not include H^+ solvation. All energy values described below include solvation effects in dichloromethane computed using the polarizable continuum model[22−24] implemented in Firefly. Natural resonance theory analysis[25−27] was performed with NBO 5.G.[28] Unless otherwise noted, all energies below are reported relative to the initial state.

Received: March 1, 2012
Published: April 24, 2012

   dx.doi.org/10.1021/jo300448d | J. Org. Chem. 2012, 77, 4653–4659

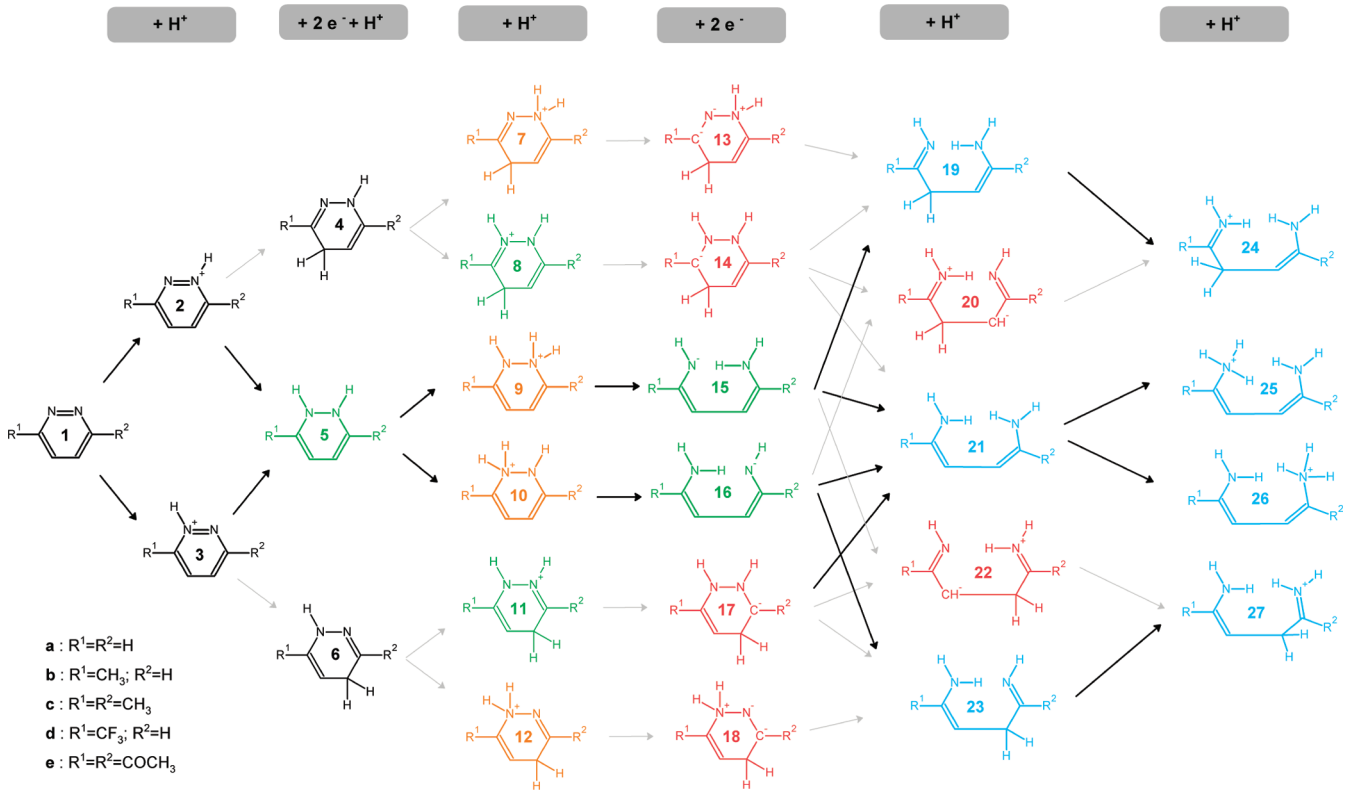

Figure 1. Possible pathways for the sequential addition of four electrons and five protons to 1,2-pyridazines. The preferred pathway for the unsubstituted pyridazine is bolded. Unproductive or highly endergonic reactions are shown as gray arrows. Molecules are color-coded according to their relative energies (black: <10 kcal·mol^{-1} top reactants; green: between 10 and 20 kcal·mol^{-1} above reactants; orange: between 20 and 30 kcal·mol^{-1} above reactants; red: >30 kcal·mol^{-11} above reactants; light blue: >15 kcal·mol^{-1} bottom reactants). Other strongly disfavored intermediates are shown in Figure 2.

RESULTS AND DISCUSSION

Reductive ring contraction of 1,2-pyridazines is usually performed in the presence of concentrated acetic or trifluoroacetic acid with a 3- to 10-fold excess of finely ground Zn dust.[9,29] Since the computational investigation of such electron-transfer reactions between metals and organic substrates is very challenging (as it entails the constraining of the orbital occupancies along reaction coordinates that lack major nuclear displacements) we analyzed the order of the reduction/protonation events by comparing the energies of the two- (or four-) electron-reduced substrate (with or without protons donated by acetic or trifluoroacetic acid) with the energies needed to remove two electrons from Zn. For these computations, we needed to compute the deprotonation energies of acetic acid (288.6 kcal·mol^{-1}) and trifluoroacetic acid (273.8 kcal·mol^{-1}), as well as the energy needed to oxidize Zn. The latter depends on the size of the Zn cluster model: removing two electrons from the bare Zn atom requires 293.2 kcal·mol^{-1} in the chosen solvent (dichloromethane) but decreases to only 210.3, 190.2, or 195.2 kcal·mol^{-1} for clusters with (respectively) four, five, or six zinc atoms. Although the precise size of the Zn clusters in the experiment is not known, we used the lower value above (190.2 kcal·mol^{-1}) as an estimate for this energy. The lack of a precise value obviously prevents the obtention of rigorous values for the energies of the electron-transfers from zinc to the substrate, but the order of the reduction/protonation events can nonetheless be ascertained with confidence. Due to the complexity of the mechanism, the reduction and protonation steps for 1,2-pyridazine will first be described and compared to several 3,6-disubstituted pyridazines. The steps involved in the actual ring closure will be described in a later section.

Reduction and Protonation of Unsubstituted 1,2-Pyridazine. Our computations show that the two-electron reduction of the unsubstituted 1,2 pyridazine (**1a**) by zinc is thermodynamically unfavorable by 129 kcal·mol^{-1}. This observation implies that reduction can only occur after the substrate is suitably activated by acquiring additional protons. Since several different possibilities for the sequential addition of four electrons and five protons to 1,2-pyridazines are possible, we analyzed all intermediates of the possible pathways (Figure 1 and Table 1) to ascertain their relative stabilities.[30] Protonation of **1a** by trifluoroacetic acid yields the trifluoroacetate anion and the monoprotonated 1,2-pyridazine, **2a** (which is equal to **3a** due to the symmetry of the substitution pattern around the ring in this instance). The reaction is only slightly disfavored thermodynamically (ΔG = 9.8 kcal·mol^{-}). A second protonation is not feasible, as the generation of that intermediate, **28a** (Figure 2), from **1a** and TFA has a sizable ΔG of 62.3 kcal·mol^{-1}. Additional protonations are still farther out of reach (ΔG = 207.7 kcal·mol^{-1} for the triply protonated state, **30a**, and 390.6 kcal·mol^{-1} for the quadruply protonated state, **31a**). Reduction of the singly protonated structure (**2a**) would yield intermediate **33a**, but this outcome is prevented due to the high energy of the resulting products (52.3 kcal·mol^{-1} above reactants). Since neither individual protonation events nor reduction events are possible, these results suggest that progression of the reaction can only occur if the two-electron reduction occurs at the same time as the inclusion

dx.doi.org/10.1021/jo300448d | J. Org. Chem. 2012, 77, 4653−4659

Table 1. Energies (in kcal·mol^{-1}, vs Isolated Reactants) of the Most Relevant Molecules Described in This Work (Complete Data Are Available as Supporting Information)

	substitutents				
	a	b	c	d	e
1	0.0	0.0	0.0	0.0	0.0
2	9.8	8.4	6.0	16.7	13.2
3	= 2	7.5	= 2	19.4	= 2
4	1.3	1.2	1.8	−3.3	−10.5
5	14.2	14.4	14.8	8.0	0.5
6	= 4	1.9	= 4	−1.4	= 4
7	= 12	19.5	= 12	27.9	= 12
8	15.1	12.0	12.3	23.1	8.9
9	= 10	27.6	= 10	31.8	= 10
10	28.5	28.4	28.0	32.0	15.4
11	= 8	15.4	= 8	17.9	= 8
12	21.7	21.7	19.6	27.0	15.0
13	= 18	122.2	= 18	87.8	= 18
14	= 17	84.2	= 17	51.1	= 17
15	= 16	17.7	= 16	3.8	= 16
16	14.2	17.6	20.9	3.0	−12.5
17	81.6	83.8	86.3	73.7	22.9
18	119.4	121.7	124.4	103.4	62.2
19	−25.2	−24.1	−23.4	−26.5	−35.3
20	54.8	57.8	58.7	36.4	7.3
21	−27.2	−25.6	−23.7	−32.2	−44.6
22	= 20	55.6	= 20	−14.7	= 20
23	= 19	−23.5	= 19	−25.7	= 19
24	−19.4	−23.1	−22.2	−10.2	−22.2
24 TS	−15.1	−15.2	−14.8	−5.6	−18.2
25	−17.6	−16.5	−15.7	−15.7	−30.4
25 TS	35.0	37.1	38.8	40.6	18.1
26	= 25	−17.0	= 25	−17.6	= 25
26 TS	= 25 TS	37.1	= 25 TS	30.4	= 25 TS
27	= 24	−18.3	= 24	−19.8	= 24
27 TS	= 24 TS	−16.6	= 24 TS	−18.6	= 24 TS
40	−19.1	−15.9	−16.0	−13.9	−20.0
41	−21.2	−18.1	−18.5	−14.9	−25.7
41 TS	−18.4	−17.5	−17.9	−12.1	−19.9
42	−22.4	−27.5	−28.0	−12.2	−26.3
42 TS	−23.2	−26.2	−26.2	−11.9	−31.7
43	−39.3	−37.5	−35.2	−39.6	−62.4
45	= 40	−19.6	= 40	−17.8	= 40
46	= 41	−21.6	= 41	−22.6	= 41
46 TS	= 41 TS	−19.0	= 41 TS	−17.3	= 41 TS
47	= 42	−22.7	= 42	−17.6	= 42
47 TS	= 42 TS	−24.1	= 42 TS	−20.5	= 42 TS

of an additional proton. This second proton may add to the same nitrogen atom as the initial proton (**34a**), to the other nitrogen (**5a**), or to the (in this case equivalent) 4- or 5-positions in the ring (**4a** or **6a**, respectively), yielding a dihydropyridazine. The least stable of these intermediates is **34a** (14.4 kcal·mol^{-1} above **5a**, which itself lies 13.0 kcal·mol^{-1} above **4a**/**6a**). Generation of **4a**/**6a** from **2a**, zinc, and TFA is favorable by 8.5 kcal·mol^{-1}.

Further reduction of **5a** or **4a**/**6a** by zinc is prohibitively expensive, as the reactions leading to the corresponding products have very large ΔG (155.4 kcal·mol^{-1} for the reaction leading to **36a** from **5a**, and 156.5 kcal·mol^{-1} for that leading to **35a** from **4a**). Natural resonance theory analysis shows that in both instances this is due to the high weight (~60%) of

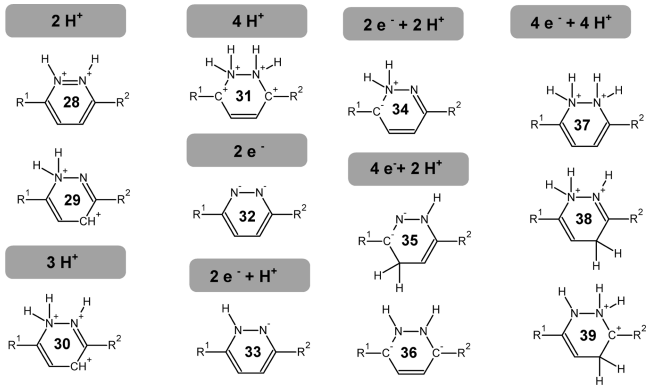

Figure 2. Unstable intermediates arising from different sequences of protonation/reduction events.

resonance structures bearing two negative charges in consecutive atoms. It is clear from these data that the second reduction step must be preceded by steps that "dilute" these negative charges, i.e., by protonation events.

Protonation of **4a**/**6a** may occur either at the "free" nitrogen atom or at the nitrogen atom that already bears a hydrogen: the latter option yields an intermediate (**7a**/**12a**) that lies 6.6 kcal·mol^{-1} above the intermediate (**8a**/**11a**) arising from the former option. Proton addition to one of the nitrogens of **5a** yields an intermediate (**9a**/**10a**) that lies 6.8 kcal·mol^{-1} above the **7a**/**12a** and 13.4 kcal·mol^{-1} above the preferred **8a**/**11a** intermediate. Further protonation of any of these intermediates generates very unstable intermediates: **37a**, **38a** and **39a** are (respectively) 54.7, 53.3, and 62.8 kcal·mol^{-1}, more acidic than trifluoroacetic acid, and cannot therefore be generated using trifluoroacetic acid as the proton donor. Interestingly, two-electron reduction of both most-favored intermediates (**8a**/**11a** or **7a**/**12a**) is not feasible (reaction ΔG of 66.4 and 97.7 kcal·mol^{-1}, respectively) as the respective products (**18a** and **13a**) bear significant charges on electropositive or on contiguous atoms. On the other hand, two-electron reduction of the (least-favored) intermediate **9a**/**10a** by zinc is favored by 14.3 kcal·mol^{-1} in a reaction that entails the breaking of N−N bond. This intermediate (**16a**) must then acquire two more protons before the ring contraction itself may occur. The first of these protons is about equally likely to add to the negatively charge nitrogen (reaction ΔG = −41.5 kcal·mol^{-1}) or to the carbon atom two bonds away from this nitrogen (reaction ΔG = −39.5 kcal·mol^{-1}). Attempts to close the neutral four-electron-reduced ring **21a** yielded very high energy intermediates (>50 kcal·mol^{-1} above **21a**). These results highlighted the need for an additional protonation before ring closure might occur. This final protonation may yield either an intermediate (**25a**) with a triply protonated nitrogen (17.6 kcal·mol^{-1} below the initial reactant state) or an intermediate with doubly protonated nitrogens (**24a**) which lies 1.8 kcal·mol^{-1} below **25a**.

Reduction and Protonation of Substituted 1,2-Pyridazines. Two pyridazines substituted with electron-donating groups, 3-methyl-1,2-pyridazine (**1b**) and 3,6-dimethylpyridazine (**1c**), and two pyridazines bearing electron-withdrawing substitutents, 3-trifluoromethyl-1,2-pyridazine (**1d**) and 1,1′-pyridazine-3,6-diyldiethanone (**1e**), were also studied. The reaction profiles of derivatives **1b** and **1c** are almost indistinguishable from the reaction profile of unsubstituted pyridazine **1a** (Figure 3), with the least stable

dx.doi.org/10.1021/jo300448d | J. Org. Chem. 2012, 77, 4653−4659

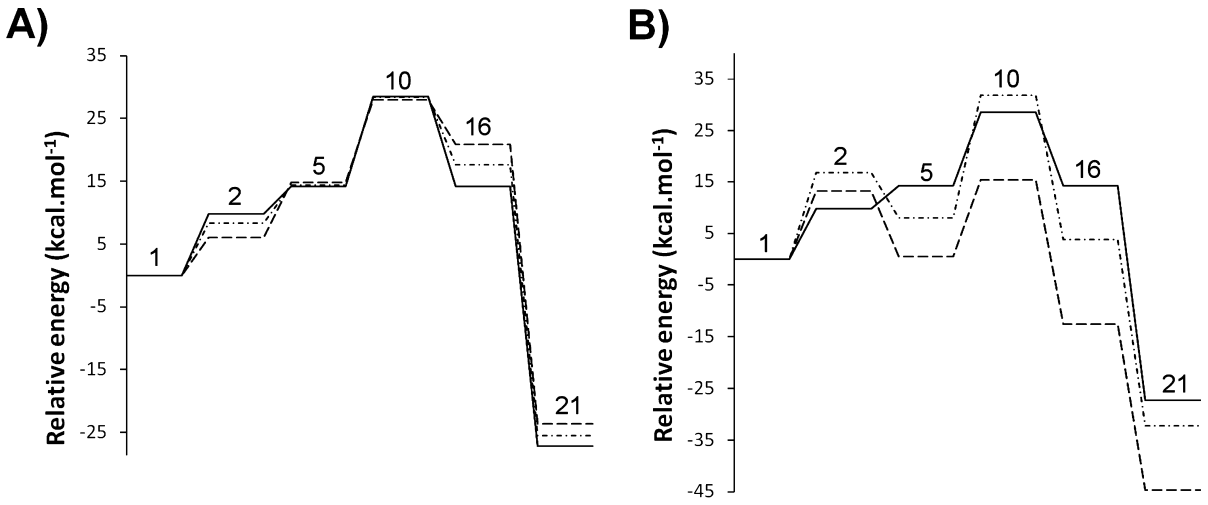

Figure 3. Comparison of the reaction profiles of pyridazine derivatives. (A) Pyridazine (**1a**, continuous line), 3-methyl-1,2-pyridazine (**1b**, dotted/broken line), and 3,6-dimethylpyridazine (**1c**, broken line). (B) Pyridazine (**1a**, continuous line), 3-trifluoromethyl-1,2-pyridazine (**1d**, dotted/broken line), and 1,1′-pyridazine-3,6-diyldiethanone (**1e**, broken line). Numerical values in the graphs identify the intermediates.

intermediate (**10**) lying ∼28 kcal mol^{-1} from the reactant state in all cases. The only relevant differences are the small stabilization of intermediate **2** (and destabilization of **16** and **21**) as the number of attached methyl groups increases. These effects can be easily rationalized by considering the well-known electron-donating effect of the methyl groups, which stabilizes intermediate **2** by decreasing the positive charge present on the nitrogen atom and destabilizes intermediates **16** and **21** by increasing the accumulation of localized negative charges. In agreement with this interpretation, we also notice that intermediate **3b**, which bears the proton on nitrogen proximal to the methyl group (and therefore is more prone to have its positive charge decreased by the electron-donating effect of the methyl group) is 1 kcal·mol^{-1} more stable than the identical intermediate **2b**, which is protonated on the distal nitrogen. Since the monomethylated pyridazine **1b** is asymmetric, several other intermediates that are equivalent in the pathway of reductive contraction of symmetric pyridazines (like **4**/**6** or **7**/**12**) are distinct species in the transformation pathway of **1b**. The energy differences between isomer pairs are not, however, very large (1−2.5 kcal·mol^{-1}, except for the **8**/**11** pair, where the difference is close to 3.5 kcal·mol^{-1}).

As expected from electrostatic considerations, the introduction of a single, electron-withdrawing, trifluoromethyl group in the pyridazine scaffold (**1d**) acts in a way opposite (Figure 3B) to that observed with the introduction of one methyl group; i.e., it destabilizes positively charge intermediates (**2d** and **10d**) and stabilizes the negatively charged species. The magnitude of the effect is larger with CF_3, as the difference in electronegativities in the C−F bond is larger than that in the C−H bond, and therefore the charge distribution in the ring is more affected by CF_3 than CH_3. The *neutral* intermediate **5d** is, however, stabilized by 6 kcal·mol^{-1} relative to **5a**, pointing to an additional, nonelectrostatic, contribution: indeed, a natural resonance theory analysis shows that this stabilizing effect arises from the relatively large weights (3−5% each) of several resonance structures involving the electron pairs on the fluorine atoms and that further delocalize the electron density.

Although the full reaction sequence is thermodynamically more favorable than in the methyl-substituted derivatives, the higher energy of the **10d** intermediate (vs **10b** or **10c**) prevents the reduction and protonation sequence of **1d** from being more accessible than those of **1a**, **1b** or **1c**. Because of the large number of intermediates studied in this portion of the mechanism, our computations did not include the location of transition states between postulated intermediates; nonetheless, the 28−32 kcal·mol^{-1} energy differences between reactant state and **10** (the highest-lying intermediate in the lowest-lying reaction pathway) in the cases described allow us to infer that **1a**, **1b**, **1c**, and **1d** may only react (if at all) at very sluggish rates, as the activation energies must necessarily be at least as large as this energy difference.

The most interesting results arose in the investigation of the reductive contraction of the derivative bearing two $COCH_3$ groups (**1e**). The initial stage proceeds as expected from the moderate electron-withdrawing character of these substituents: the energy gap between **1e** and intermediate **2e** lies between the energy gaps computed for unsubstituted pyridazine and 3-fluoromethyl pyridazine. Thenceforth, the reaction acquires a very distinctive energetic profile as the $COCH_3$ substituents strongly stabilize intermediates **5e** and **10e** by 13−14 kcal·mol^{-1} (relative to **5a** and **10a**), due to sizable electron delocalization away from the ring and into the C═O moiety (Table 2). In consequence, the highest lying intermediate in the pathway (**10e**) becomes very accessible, only 15.4 kcal·mol^{-1} above the isolated reactants. The transition state for the **5e**→**10e** proton transfer is, accordingly, readily accessible (19.0 kcal·mol^{-1} above initial reactants). Generation of **10e** from **11e** through a CF_3COOH-assisted proton transfer from the C4 atom to the N1 nitrogen was found to be too slow (ΔG_{act} > 50

Table 2. Combined Resonance Weight (%) of All Resonance Structures of 5 and 10 Differing among Themselves Only on the Bonding Pattern of the Heavy Atoms of the Pyridazine Ring[a]

	substituents				
	a	**b**	**c**	**d**	**e**
5	98.5	98.6	96.1	80.9	66.2
10	98.6	97.4	96.0	78.2	66.8

[a]Hyperconjugation and resonance away from the ring are not included.

dx.doi.org/10.1021/jo300448d | J. Org. Chem. 2012, 77, 4653−4659

kcal·mol^{-1}), confirming that the pathway leading from **1**→**2**→**6**→**11** is not productive.

The intermediates after **10e** (**16e** and **21e**) also strongly benefit from the electron-withdrawing and resonant character of $COCH_3$, making the whole sequence highly exergonic. Interestingly, intermediates **17e** and **18e** are stabilized by more than 55 kcal·mol^{-1} (relative to **17a** and **18a**) but still remain either energetically inaccessible (**18e**, 62.2 kcal·mol^{-1} above reactants) or strongly disfavored (**17e**, 22.9 kcal·mol^{-1} above reactants) when compared to their **16e** isomer (12.6 kcal·mol^{-1} below reactants).

Generation of the Four-Electron-Reduced Species (15/16) through Disproportionation of the Two-Electron Reduced Species (5). The results shown in the previous section clearly show that only the $COCH_3$-disubstituted derivative may be expected to react at reasonable rates, as the elevated energies of the **10a**, **10b**, **10c**, and **10d** intermediates (28−32 kcal·mol^{-1} vs reactants) imply very slow reactions at the experimental temperatures (25 °C). However, since electrochemical investigations[14] have shown that some 1,2-pyridazines may undergo disproportionation after accepting two electrons, we decided to investigate whether disproportionation of **5** might afford more accessible pathways for the generation of the four-electron reduced intermediates **15**/**16**, thereby bypassing the high-energy **10a**−**d** intermediates. Our computations clearly showed that direct hydride transfer between two **5** molecules, yielding one **3** molecule and one **16** molecule is not possible, as the two electrons do not accompany the movement of the hydrogen nucleus. Instead, one of the **5** molecules must first be converted to an "open" form through the breaking of its N−N bond (Figure 4, panels A and C). This "open" intermediate contains three conjugated π-bonds and may abstract a hydride from the "closed" form, yielding **16** and **3** (Figure 4, panels B and D). The **16a** and **16d** derivatives immediately abstract an extra proton from **3a** and **3d**, respectively, finally yielding **1a**/**d** and **21a**/**d**. For all 1,2-pyridazines studied, the limiting step in this pathway is the breaking of the N−N bond in intermediate **5** (Table 3).

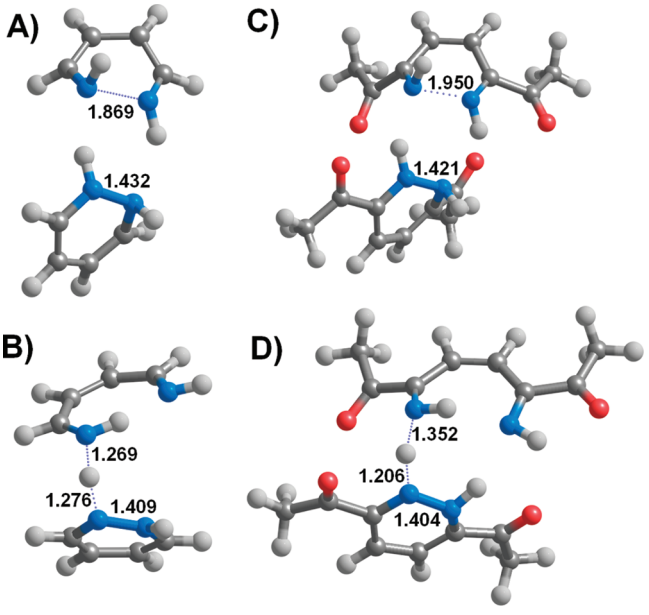

Figure 4. Transition states for the disproportionation of selected two-electron-reduced 1,2-pyridazines: (A) opening the ring at the two-electron/two-proton stage in the unsubstituted 1,2-pyridazine (**5a**); (B) hydride transfer from "closed" **5a** to "open" **5a**; (C) Opening the ring at the two-electron/two-proton stage in the $COCH_3$-disubstituted 1,2-pyridazine (**5e**); (D) hydride transfer from "closed" **5e** to "open" **5e**. Distances (in Å) between intervening atoms are depicted in bold.

Table 3. Energies (in kcal·mol^{-1} vs Two Interacting Molecules of 5) of the Intermediates in the Disproportionation Pathway[a]

	substitutents				
	a	**b**	**c**	**d**	**e**
5 + **5**	0.0	0.0	0.0	0.0	0.0
TS1	17.8	17.4	20.7	23.9	26.0
5 + "open" **5**	−15.5	−15.6	−16.4	−10.3	−2.3
TS2	−7.5	−6.4	−3.7	0.2	10.5
3 + **16**	→**1** + **21**	−20.9	−17.0	→**1** + **21**	−16.2
1 + **21**	−55.0			−46.4	

[a]For the unsubstituted (**a**) and trifluoromethyl (**d**) pyridazines, products **3** + **16** spontaneously decay into **1** + **21**.

Generation of **5** from the initial reactants is itself endergonic (see Table 1), so that this transition state (**TS1**) effectively remains too high in energy (27−34 kcal·mol^{-1} above initial, infinitely separated, reactants) for all molecules.

Other disproportionation pathways were also analyzed. Direct computation of the reaction energies from the values already obtained shows that disproportionation of two molecules of **6** to yield **17** + **3** is unfavorable by 59−90 kcal·mol^{-1}. Disproportionation of **6** into **18** + **3** is even less favorable by 95−130 kcal·mol^{-1}. In both instances, these high

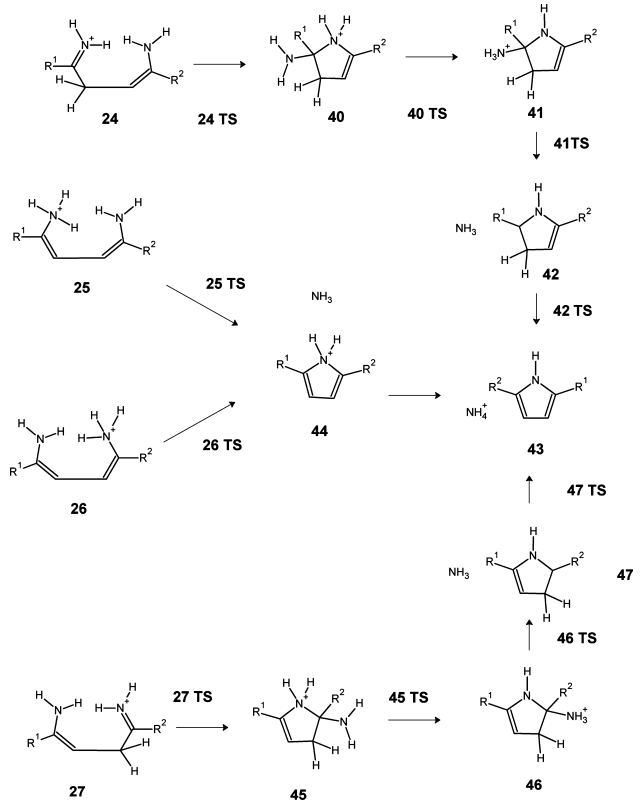

Figure 5. Pathways leading to pyrrole from four-electron-reduced/five-protons-bearing pyridazines.

dx.doi.org/10.1021/jo300448d | J. Org. Chem. 2012, 77, 4653−4659

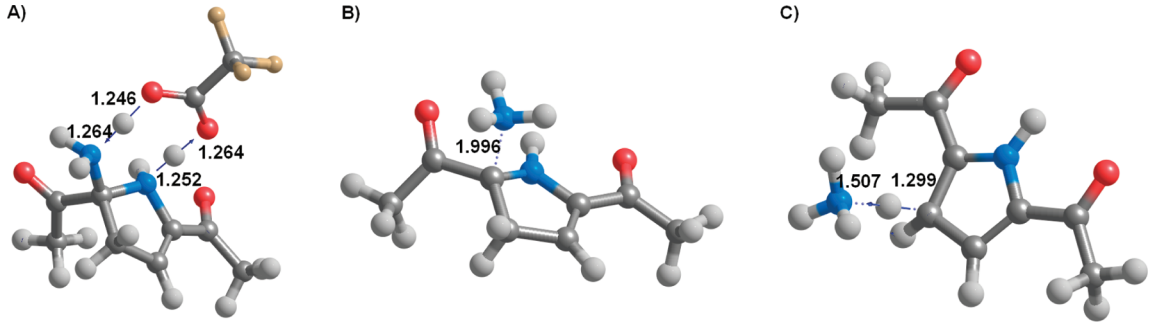

Figure 6. Transition states of the final steps of reductive ring contraction of pyridazines: (A) CF_3COOH-assisted proton transfer from the ring nitrogen to the leaving amino group (**40TS/e**); (B) NH_3 elimination (**41TS/e**); (C) aromatization (**42TS/e**). Distances (in Å) between intervening atoms are depicted in bold. Arrows show the vibrations associated with the imaginary frequencies of transition states.

energies are due to the very low stabilities of intermediates **17** and **18**. Hydride transfer from **6** to **11**, yielding **23** and **3**, is thermodynamically favorable by >20 kcal·mol^{-1} for all substituents studied, but the corresponding transition states lie >45 kcal·mol^{-1} above reactants in all cases.

Pyrrole Formation. For all pyridazines studied, the most stable product obtained after adding four electrons and four protons to pyridazine is intermediate **21**. Generation of intermediates **19**/**23**, however, is also very exergonic, and it is therefore very likely that the final protonation occurs on any of these intermediates, leading to the production of a mixture of intermediates **24**−**27** (Table 1). The putative pathways leading to pyrrole from these intermediate are shown in Figure 5.

Our computations show that conversion of **25**/**26** to **44** is not at all feasible at room temperature for any of the tested pyridazine derivatives, as the activation energies always exceed 45 kcal·mol^{-1}. In contrast, the pathway that begins with intermediates **24**/**27** is very fast for all pyridazines studied: the barrier height for conversion of **24** to **40** ranges from 4.0 kcal·mol^{-1} (**24e**→**40e**) to 7.9 kcal·mol^{-1} (**24b**→**40b**). In the monosubstituted derivatives, conversion of **27** to **45** occurs with even lower barriers, of 1.8 kcal·mol^{-1} (**27b**→**45b**) or 1.2 kcal·mol^{-1} (**27d**→**45d**).

Since NH_2 is not a good leaving group, the transfer of a proton to this group is now required. This (exergonic) reaction can be performed very elegantly with the assistance of one molecule of trifluoroacetic acid, which simultaneously protonates the amino group and deprotonates the ring nitrogen (Figure 6) with a very small barrier of 1.8 kcal·mol^{-1} (**40e**→**41e**). NH_3 then leaves the ring very easily, leaving a positive charge behind (intermediate **42**). Except in the derivative bearing an electron-withdrawing CF_3 substituent, this step is moderately exergonic (−0.7 to −9.5 kcal·mol^{-1}). Removal of the final proton from the ring may be performed by the basic NH_3 just evicted from the molecule, in a very exergonic step that restores the aromaticity of the system. Although we could find the transition states (**42TS**/**47TS**) in the electronic energy surface for this step in all molecules studied, inclusion of zero-point energy and vibrational contributions to enthalpy and entropy lowers their energies below those of the corresponding reactants (**42**/**47**). This step is therefore expected to occur without a barrier and to be effectively diffusion-controlled.

CONCLUSIONS

Reductive ring contraction of 1,2-pyridazines using Zn/TFA follows a sequential mechanism whose rate seems to be limited by the addition of the third proton to the two-electron-reduced species. The high energy of this $2e^-/3H^+$-bearing intermediate slows the reaction rates, unless positions 3- and 6- of the pyridazine ring bear substituents able to resonate negative charge away from the ring. The same substituent effects are also observed in an alternative pathway (which proved equally ineffective) involving disproportionation of earlier $2e^-/2H^+$-bearing intermediates to bypass this unfavorable $2e^-/3H^+$-bearing intermediate. The character of the ring substituents does not, however, greatly affect the outcome of the ring contraction steps, which have very small barriers in all cases studied. By establishing the need for electron-withdrawing resonant groups in the 3- and 6- positions, this work suggests that the reductive ring contraction of 1,2-pyridazines may be applied to pyridazines bearing $COCH_3$ groups, amides or aryls in these positions, further expanding the scope of this interesting synthetic route, nowadays applied mostly to 3,6-dicarbomehoxy-1,2 pyridazines[8−12] and 3,6-bipyrydyl-1,2-pyridazines.[14] Finally, the 1,4-dihydropyridazine intermediate (**4**/**6** in our scheme) found in electrochemical investigations[13,14] and isolated in the course of the total synthesis of *ent*-(−) roseophilin[9] seems to be part of an unproductive pathway involving (at the four-electron-reduced stage) intermediates (**17** or **18**) with energies far above those on the preferred pathway.

ASSOCIATED CONTENT

Supporting Information

Geometries and energies of every molecule described. This material is available free of charge via the Internet at http://pubs.acs.org.

AUTHOR INFORMATION

Corresponding Author

*E-mail: pedros@ufp.edu.pt.

Notes

The authors declare no competing financial interest.

ACKNOWLEDGMENTS

Research at REQUIMTE is supported by Fundação para a Ciência e a Tecnologia through Grant No. PEst-C/EQB/LA0006/2011.

REFERENCES

(1) Knorr, L. *Chem. Ber.* **1884**, *17*, 1635.
(2) Hantzsch, A. *Chem. Ber.* **1890**, *23*, 1474.
(3) Paal, C. *Chem. Ber.* **1884**, *17*, 2756.
(4) Knorr, L. *Chem. Ber.* **1884**, *17*, 2863.

(5) Dhawan, R.; Arndtsen, B. A. *J. Am. Chem. Soc.* **2004**, *126*, 468.
(6) Joshi, U.; Pipelier, M.; Naud, S; Dubreuil, D. *Curr. Org. Chem* **2005**, *9*, 261−288.
(7) Bach, N. J.; Kornfeld, E. C.; Jones, N. D.; Chaney, M. O.; Dorman, D. E.; Paschall, J. W.; Clemens, J. A.; Smalstig, E. B. *J. Med. Chem.* **1980**, *23*, 481.
(8) Boger, D. L.; Coleman, R. S.; Panek, J. S.; Yohannes, D. *J. Org. Chem.* **1984**, *49*, 4405.
(9) Boger, D. L.; Hong, J. *J. Am. Chem. Soc.* **2001**, *123*, 8515−8519.
(10) Hamasaki, A.; Zimpleman, J. M.; Hwang, I.; Boger, D. L. *J. Am. Chem. Soc.* **2005**, *127*, 10767.
(11) Liangfeng, F.; Gordon, W. G. *Tetrahedron Lett.* **2010**, *51*, 537.
(12) Oakdale, J. S.; Boger, D. L. *Org. Lett.* **2010**, *12*, 1132.
(13) Manh, G. T.; Hazard, R.; Pradère, J. P.; Tallec, A.; Raoult, E.; Dubreuil, D. *Tetrahedron Lett.* **2000**, *41*, 647.
(14) Manh, G. T.; Hazard, R.; Pradère, J. P.; Tallec, A.; Raoult, E.; Dubreuil, D.; Thiam, M.; Toupet, L. *Electrochim. Acta* **2002**, *47*, 2833.
(15) Becke, A. D. *J. Chem. Phys. I* **1993**, *98*, 5648.
(16) Lee, C.; Yang, W.; Parr, R. *J. Phys. Rev. B* **1998**, *37*, 785.
(17) Hertwig, R. W.; Koch, W. *J. Comput. Chem.* **1995**, *16*, 576.
(18) Baker, J.; Kessi, A.; Delley, B. *J. Chem. Phys.* **1996**, *105*, 192.
(19) Stevens, W. J.; Krauss, M.; Basch, H.; Jasien, P. G. *Can. J. Chem.* **1992**, *70*, 612−630.
(20) Granovsky, A. A. Firefly version 7.1.G, http://classic.chem.msu.su/gran/gamess/index.html.
(21) Schmidt, M. W.; Baldridge, K. K.; Boatz, J. A.; Elbert, S. T.; Gordon, M. S.; Jensen, J. J.; Koseki, S.; Matsunaga, N.; Nguyen, K. A.; Su, S.; Windus, T. L.; Dupuis, M.; Montgomery, J. A. *J. Comput. Chem.* **1993**, *14*, 1347.
(22) Tomasi, J.; Persico, M. *Chem. Rev.* **1994**, *94*, 2027−2094.
(23) Mennucci, B.; Tomasi, J. *J. Chem. Phys.* **1997**, *106*, 5151−5158.
(24) Cossi, M.; Mennucci, B.; Pitarch, J.; Tomasi, J. *J. Comput. Chem.* **1998**, *19*, 833−846.
(25) Glendening, E. D.; Weinhold, F. *J. Comput. Chem.* **1998**, *19*, 593−609.
(26) Glendening, E. D.; Weinhold, F. *J. Comput. Chem.* **1998**, *19*, 610−627.
(27) Glendening, E. D.; Badenhoop., J. K.; Weinhold, F. *J. Comput. Chem.* **1998**, *19*, 628−646.
(28) Glendening, E. D.; Badenhoop, J. K.; Reed, A. E. ; Carpenter, J. E.; Bohmann, J. A.; Morales, C. M.; Weinhold, F., 2004, NBO 5.G, Theoretical Chemistry Institute, University of Wisconsin, Madison, WI, 2004; http://www.chem.wisc.edu/∼nbo5.
(29) Boger, D. L.; Panek, J. S.; Patel, M. *Org. Synth.* **1992**, *70*, 79.
(30) For simplicity, some "dead-end" intermediates are not depicted in Figure 1. They are shown in Figure 2 and discussed briefly in the text.